ELSEVIER

Journal of Chromatography A, 786 (1997) 171–180

JOURNAL OF CHROMATOGRAPHY A

Salt effects in capillary zone electrophoresis I. Dependence of electrophoretic mobilities upon the hydrodynamic radius

Reginald F. Cross*, Jing Cao

School of Chemical Sciences, Swinburne University of Technology, John Street, Hawthorn, Vic. 3122, Australia

Received 4 December 1996; received in revised form 14 May 1997; accepted 14 May 1997

Abstract

An examination of the derivation of the equation relating electrophoretic mobility (μ_{ep}) to charge and the hydrodynamic radius (r) shows that the $1/r$ dependence arises from an approximation. A more generalised approach yields a $1/r^2$ dependence and includes the known $1/\sqrt{I}$ dependence as well. Nine totally ionised sulphonamides have been used to test the proposed relationship between μ_{ep} and r, and at each of four buffer concentrations utilised the correlations favour $1/r^2$. For large molecules, μ_{ep} has frequently been demonstrated to be proportional to $1/M_r^{2/3}$, which can be equivalent to $1/r^2$. However, it has been suggested that there may be a transition from $1/r$ dependence for small molecules to a $1/r^2$ dependence for large molecules. Hence we have used literature data for a series of twenty-two peptides varying in size between 3 and 39 amino acids long to test that theory and the generality of the $1/r^2$ dependence. The calculations indicate a consistent dependence upon $1/r^2$. © 1997 Elsevier Science B.V.

Keywords: Salt effects; Electrophoretic mobility; Hydrodynamic radius; Sulfonamides; Peptides

1. Introduction

The electrophoretic mobility (μ_{ep}) of an analyte is frequently described by the fundamental relationship of Eq. (1):

$$\mu_{ep} = \frac{Z}{6\pi\eta r} \quad (1)$$

where Z is the effective charge on the ion, η is the viscosity and r is the hydrodynamic radius. Eq. (1) is intuitively satisfactory as increased charge causes greater mobility and the bigger the ion or the more viscous the medium through which it moves, the larger the viscous drag and the less mobile the ion.

Various tests have confirmed the dependence upon Z shown in Eq. (1). For example, a good correlation ($R=0.985$) was found between the observed mobilities of eighteen sulphonamides (SFAs) and the so-called "charge-to-mass" ratios calculated from pK_a data and known molecular masses (M_r values) [1]. As the SFAs are relatively homogeneous in composition and shape, the volumes of the molecules will be closely related to their M_r values. However, the use of "charge-to-mass" ratios and M_r is a crude test of Eq. (1), at best. Firstly, there is the presumption of direct proportionality between size and molecular mass. In the case of an examination of a

*Corresponding author.

0021-9673/97/$17.00
PII S0021-9673(97)00547-5

series of similarly sized and shaped dihydrofolate reductase inhibitors (DHFRIs), it became immediately obvious that the behaviour of one of the eight DHFRIs was strongly discordant with the correlation observed between electrophoretic mobilities and the "charge-to-mass" ratios for the other seven. The high atomic mass of a bromine atom in the one compound was the cause [2].

The second problem with the use of "charge-to-mass" or "charge-to-volume" ratios is that in Eq. (1) μ_{ep} is inversely proportional to r, not molecular volume (V_r) or M_r. In fact there are three presumptions even in the use of "equivalent" functions of M_r and V_r in the place of r. (i) If the atomic mass distribution in a series of molecules is the same, then the average mass per atom is the same and M_r is proportional to the number of atoms. (ii) If these atoms are also arranged in the same relativity (basic shape and conformation), the molecular densities will be the same and V_r will become proportional to M_r. (iii) Therefore, if we assume that a molecule may be represented by a sphere of "equivalent volume", V_r ($=4/3\pi r^3$)$\propto M_r$ and $r \propto M_r^{1/3}$. Indeed Weinberger [3] has suggested that μ_{ep} is better related to $M_r^{1/3}$ than other functions of M_r, for small molecules. We have used molecular modelling to determine optimum configurations of eight DHFRIs, and from these the surface areas of the hydrated molecules and thus r values for equivalent spheres. The correlation was again good ($R=0.980$), but in that case between μ_{ep} and Z/r [2]. At first sight, these two correlations may appear to be in conflict. But in the case of the SFAs, in effect there was only a correlation between μ_{ep} and Z since the charges varied from 0.0001 to 1 while the M_r was generally 265 ± 10. For the DHFRIs, the situation was similar. Interestingly, whilst the ultimate separation of identically charged ions was certainly due to subtle differences in size [4], the correlation between μ_{ep} and Z/r was little affected by this factor. In effect then, both of these studies [1,2] have supported $\mu_{ep} \propto Z$, but have not tested $\mu_{ep} \propto 1/r$.

For large molecules several studies have correlated μ_{ep} with $Z/M_r^{2/3}$ [5–10]. The correlations are good, and in the case of estimates of Z based upon substrate-specific pK_a data – rather than the use of isolated amino acid pK_a data in peptides (where charge suppression is known to occur) – the correlation was extremely tight [10]. Again, $\mu_{ep} \propto Z$ is clearly supported. Given the composition and size of (larger) peptides and proteins, the proportionality between molecular mass and molecular volume may be valid. Hence the cube roots of M_r values provide relative radii of equivalent spheres and the squares of these provide relative surface areas. Thus μ_{ep} is shown to be dependent upon the surface area and not the radius to the power of one.

Compton [11] has suggested that there is a transition between electrophoretic behaviour of small molecules ($\mu_{ep} \propto 1/r$) and large molecules ($\mu_{ep} \propto 1/r^2$). Assuming Eq. (1) as the starting point, after the introduction of the Henry correction: $\mu_{ep} = k1 \cdot Z/(k2 \cdot M_r^{1/3} + k3 \cdot M_r^{2/3} \cdot I^{1/2})$.

Calculations then indicated the predominance of the $k2 \cdot M_r^{1/3}$ term for small molecules at low ionic strength (I) but of the $k3 \cdot M_r^{2/3} \cdot I^{1/2}$ term for large molecules at high ionic strength ($k1$, $k2$ and $k3$ are constants defined in Ref. [11]). Weinberger [3] has also indicated that the empirical model produced by Grossman et al. [12] fits between these two extremes of behaviour. As these authors examined μ_{ep} for peptides containing between 3 and 39 amino acids with formal charges ranging from 1.3 to 14.3, these analytes certainly provide a good test of any proposed dependencies of μ_{ep} upon Z and (M_r or r). However, no such tests appear to have been done. Furthermore, in our examinations of correlations between μ_{ep} and molecular variables for small molecules, we have observed stronger correlations between μ_{ep} and Z/r^x where x is 2 or 3, rather than 1.

An additional factor concerns the effect of buffer concentration; ionic strength. Weime [13,14] has suggested that μ_{ep} should be proportional to $1/\sqrt{I}$ and Issaq et al. [15] have provided experimental verification. This is consistent with our own observations at low values of ionic strength [4,16].

The above factors lead to the question of the validity of the basic form of Eq. (1). In this paper we present an examination of the theory relating to the derivation of Eq. (1) and experimental data to test the outcomes. We also re-examine the data of Grossman et al. [12].

2. Theory

The dependence of the electrophoretic mobility

(μ_{ep}) upon the zeta-potential was derived by Huckel by correcting the Stokes' Eq. for the electrophoretic retardation of the immediate ionic atmosphere. Henry [17] has verified this relationship, and in rationalised SI units [18] it is (Eq. (2)):

$$\mu_{ep} = \frac{2\varepsilon_r \zeta}{3\eta} \tag{2}$$

where ε_r is the relative permittivity of the solution, η is the viscosity of the buffer and ζ is the zeta-potential; the potential drop from the solid–liquid interface to the slipping plane.

The zeta-potential [18–21] is related to the thickness of the double layer, δ, as shown by Eq. (3):

$$\zeta = \frac{\delta\sigma_0}{\varepsilon_r} \tag{3}$$

provided the surface potential is small [21]. σ_0 is the total excess charge per unit surface area. For most analytes the charge per unit surface area is problematic, and for the SFAs used in this study as test analytes at pH 7, the negative charge on the deprotonated N will not be highly delocalised. However, taking the simplest approximation of $Z/4\pi r^2$ and combining it with Eqs. (2) and (3) yields Eq. (4):

$$\mu_{ep} = \frac{Z\delta}{6\pi\eta r^2} \tag{4}$$

It is at this point that the final form of the dependence of μ_{ep} upon r is determined. If the thickness of the electrical double layer (δ) is set equal to the hydrodynamic radius of the ion (r), Eq. (4) becomes Eq. (1). And setting $\delta = r$ is not unreasonable. Provided that the sphere of hydration is chosen to be sufficiently large, the radius of the hydrated ion will extend out to the slipping plane and all of the mobile mass of analyte plus solvent will be incorporated. As long as r is adjusted in accordance with solution conditions, Eq. (1) becomes a good approximation.

An alternative is to approach the question of δ from the point of view of surface and colloid chemistry. The analogy should not be pushed too far since the surface of a solid or colloidal particle is macroscopic and is surrounded by an extended double layer of ions. We are considering single ions and their local environments. However, the concept of a double layer extending out from the surface of the ion into a diffuse region of influence is useful. As for the solid or colloidal particles, this leads to a consideration of the quantitative effect of ionic strength upon μ_{ep}.

The so-called inverse Debye–Huckel length, κ^{-1}, is commonly equated with δ in colloid chemistry [17–22]. It is a pseudo constant multiplier derived from the Debye–Huckel theory, it has the dimensions of length and is dependent upon $1/\sqrt{I}$, as required. The definition of κ [17–23] is given by Eq. (5):

$$\kappa^2 = \frac{e^2 \sum_i n_i z_i^2}{\varepsilon_r kT} \tag{5}$$

where e is the protonic charge, n_i is the number of ions i per cm^3, z_i is the valence of ions i, k is the Boltzmann constant and T the absolute temperature. At 30°C this gives $\delta = [0.330 \cdot 10^8 \sqrt{I}]^{-1}$ cm [24]. Substituting into Eq. (4) and re-arranging yields Eq. (6):

$$\mu_{ep} = \frac{Z}{6\pi\eta r^2} \cdot \frac{1}{3.30 \cdot 10^7 \sqrt{I}} \tag{6}$$

Eq. (6) has been written as two parts to demonstrate the modification of Eq. (1) that occurs when δ is set equal to κ^{-1}.

3. Experimental

3.1. Instrumental

A Model 270A CE System by Applied Biosystems (Foster City, CA, USA) was used for all capillary zone electrophoresis (CZE) experiments. The analytes were detected by UV–Vis absorbance at 254 nm and the detector time constant was set at 0.3 s in all experiments.

The determinations were performed on a 67.3 cm×50 μm I.D.×220 μm O.D. fused-silica capillary (Applied Biosystems) with the detection window located 49.0 cm from the injection end. Vacuum injection took place at the anode (+) and all experiments were performed at 30°C and 18 kV. Electropherograms were recorded on a DeskJet Plus recorder and data were collected and integrated with

a Model 270 CE system interfaced to an Apple Macintosh computer.

3.2. Chemicals and materials

The sulphonamides used in the study were obtained from Sigma (St. Louis, MO, USA). The nine compounds and their pK_a values were, respectively, sulphaquinoxaline (SQ) 5.5, sulphachloropyridazine (SCP) 5.5, sulphabenzamide (SBE) 4.6, sulphamethoxazole (SMOZ) 5.6, sulphisoxazole (SIOX) 5.1, sulphamethizole (SMI) 5.4, sulphacetamide (SAC) 5.4, phthalyl sulphacetamide (PSAC) ~2.89 and 5.4, and sulphanilic acid (SA) 3.2.

Standard stock solutions of each compound were prepared by precisely dissolving 0.1 g in 100 ml of HPLC-grade methanol (BDH). Each compound was diluted with Milli-Q water to give a final concentration of 25 ng/μl. Sample solutions were filtered (0.45 μm) before injection. The sodium phosphate buffers were 65, 101, 174 and 210 m*M* with respect to phosphate and were prepared from Na_2HPO_4 and NaH_2PO_4 by calculation of the exact amounts required according to the Henderson–Hasselbach equation. Precise masses per unit volume were then dissolved in water to just short of the required total volume. These solutions were then magnetically stirred and the stable pH recorded relative to a freshly prepared pH 7 commercial standard. Where the pH was slightly outside of the range of 7.00±0.05, a small number of drops of 20% H_3PO_4 or 0.1 *M* NaOH were added with thorough stirring to obtain the desired pH of 7.0. Chemicals were of analytical-reagent grade and Milli-Q water was used to prepare all solutions.

3.3. Methods

Capillary preparation at the start of each day of experimentation involved initial purging with 0.1 *M* NaOH for 3 min, followed by Milli-Q water purging for 3 min and then the running buffer for 3 min. Between runs, the capillary was purged with 0.1 *M* NaOH for 3 min followed by running buffer for 3 min. Vacuum injections of 7 s duration were used. At the nominal 4 nl/s [25], 28 nl would have been injected. However, the more viscous buffers used would lead to greatly reduced injection volumes. Furthermore, as the sample was dissolved in water, sample stacking compensated for this larger than usual volume. Electroosmotic mobilities were determined by the appearance of the baseline disturbance due to the methanol solvent.

4. Results and discussion

The first feature of Eq. (6) is that $\mu_{ep} \propto 1/\sqrt{I}$. This is a dependence that has been discussed by others [26,13–15] and has been clearly demonstrated experimentally by Issaq et al. [15]. However, as these authors point out, there is far from universal agreement. From our own data on the DHFRIs [4] and SFAs [16], this dependence appears to be correct at low to moderate buffer concentrations. Under these conditions, Joule heating, changes to ionisation of the analytes due to salt effects and the synergism between these two effects will be minimal [16]. We have not attempted to test this dependence any further and as we are concerned with CE analyses in high buffer concentrations, the data presented in this paper cannot be simply analysed to discern the component that is due to increases in ionic strength from that due to Joule heating [16].

The second feature of Eq. (6) is that $\mu_{ep} \propto 1/r^2$. This is in conflict with the generally accepted dependence of Eq. (1), but is in accordance with the findings for larger molecules where $\mu_{ep} \propto 1/M_r^{2/3}$ [5–10].

4.1. Testing Eqs. (1) and (6)

Table 1 shows the raw and calculated data used to investigate the applicability of Eqs. (1) and (6) with respect to the dependence of μ_{ep} upon r. This was done via the correlation between the measured μ_{ep} (in 174 m*M* buffer, column 8), and Z/r (column 5) and Z/r^2 (column 6). Z/r^3 is also included (column 7).

The charges were calculated from the pK_a data given in Section 3.2 and are shown in column 3. For each charged site on each SFA, one water of solvation has been allocated. These are shown in column 2. As in the previous study [2], we applied the Sybyl 6.01 molecular modelling software to built up minimum energy configurations of the nine SFAs

Table 1
Charge, radius, calculated relative mobilities and measured electrophoretic mobilities in 174 m*M* sodium phosphate buffer at pH 7

Migration order	SFA·nH_2O	Charge (Z)	Radius (r, Å)	Relative mobilities			Electrophoretic mobilities ($cm^2 \cdot 10^{-5}$/V s)
				Z/r	Z/r^2	Z/r^3	
1	SQ·H_2O	−0.969	3.817	−0.2539	−0.0665	−0.0174	−22.600
2	SCP·H_2O	−0.969	3.659	−0.2648	−0.0724	−0.0198	−23.252
3	SBE·H_2O	−0.996	3.728	−0.2672	−0.0717	−0.0192	−23.705
4	SMOZ·H_2O	−0.962	3.607	−0.2667	−0.0739	−0.0205	−24.155
5	SIOX·H_2O	−0.988	3.817	−0.2588	−0.0722	−0.0178	−24.587
6	SMI·H_2O	−0.976	3.676	−0.2655	−0.0678	−0.0196	−24.934
7	SAC·H_2O	−0.976	3.435	−0.2841	−0.0827	−0.0241	−27.122
8	PSAC·$2H_2O$	−1.976	4.061	−0.4866	−0.1198	−0.0295	−34.587
9	SA·H_2O	−1	3.195	−0.313	−0.0980	−0.0307	−36.009

with a water of hydration added to each of the ionised sites. Based on these structures, the averaged radius of an equivalent sphere was calculated from the volume of the SFAs. These are given in the fourth column of Table 1.

The plot of μ_{ep} versus Z/r is shown in Fig. 1. The solid line was obtained from linear regression, has the equation $\mu_{ep}/10^{-5} = 0.567 + 92.17\ Z/r$ and has a correlation coefficient of $R = 0.753$. Fig. 2 shows the plot of μ_{ep} versus Z/r^2. Its regression data is $\mu_{ep}/10^{-5} = -0.658 + 322.6\ Z/r^2$ and with $R = 0.908$. It is clear from Figs. 1 and 2 and the correlation coefficients that the plot versus Z/r^2 is a better fit to the data. Table 2 gives the equivalent correlation

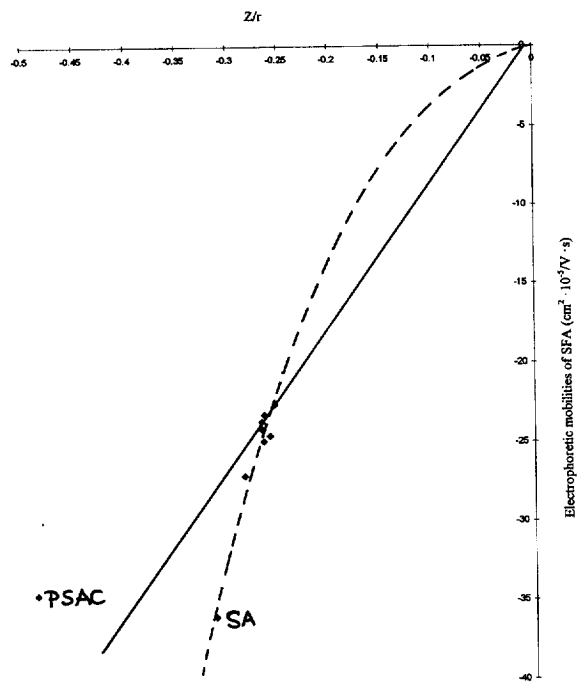

Fig. 1. Electrophoretic mobilities of the nine SFAs ($cm^2 \cdot 10^{-5}$/V s) in a 174 m*M* sodium phosphate buffer plotted versus Z/r. The solid line is the linear regression calculated from the experimental results and the dashed line is an alternative interpretation of the data (see Section 4.1).

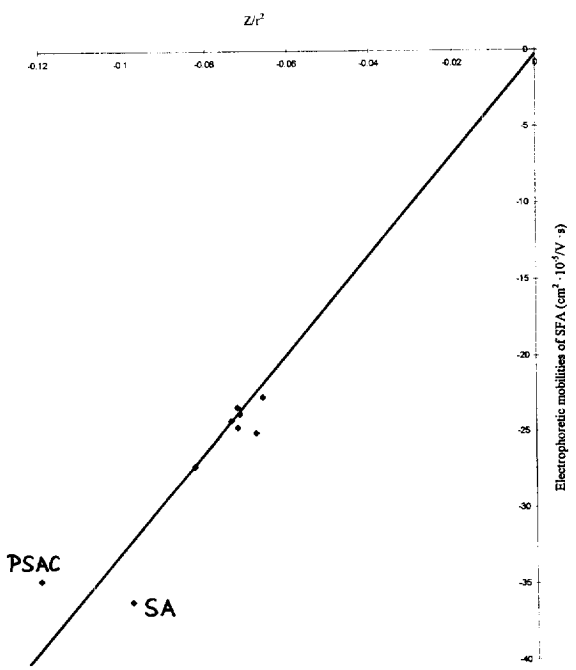

Fig. 2. Electrophoretic mobilities of the nine SFAs ($cm^2 \cdot 10^{-5}$/V s) in 174 m*M* sodium phosphate buffer plotted versus Z/r^2. The solid line is the linear regression calculated from the experimental results.

Table 2
Correlation coefficients for plots of the measured electrophoretic mobilities versus the calculated relative values Z/r, Z/r^2 and Z/r^3

Buffer concentration (mM)	Z/r	Z/r^2	Z/r^3
65	0.786	0.928	0.968
101	0.769	0.918	0.968
174	0.753	0.908	0.967
210	0.648	0.842	0.947

coefficients for the other three buffer concentrations and it is evident that the Z/r^2 plots are universally a significantly better fit. Indeed, the Z/r and Z/r^2 plots for the other three buffer concentrations are qualitatively identical to those in Figs. 1 and 2.

In the central region of the plots where the majority of the data lie, the seven similarly charged ($Z \approx 1$) and similarly shaped SFAs (see general structure, Fig. 3) are tightly bunched as expected. (With the exception of SAC, where Ar is an acetyl group, Ar represents an aromatic structure that is generally a mono-substituted heterocycle. The exact structures are given in Ref. [1]). The other two analytes are significantly different in size and structure, as is shown in Fig. 3. Although frequently grouped with other SFAs, SA is not an amide but a sulphonic acid, it lacks a second aromatic group, is by far the smallest analyte and has a mobility apparently in excess of the predicted value. By contrast, PSAC is a diamide with a very different structure, is by far the largest analyte and is far less mobile than expected relative to the other SFAs. Internal hydrogen bonding is apparent, but it is difficult to see how this would decrease its mobility. The μ_{ep} of these two analytes (SA, PSAC) are widely divergent from the line of best fit in the case of Fig. 1 and are clearly the reason for the poorer correlation. An alternative interpretation of the data in Fig. 1 is given by the dashed line through the seven SFAs other than PSAC. It is a tight fit through the data points, passes comfortably through the origin and indicates a higher order dependence upon r. To test the validity of this interpretation (dashed line), Z/r^2 is plotted versus Z/r in Fig. 4. The distribution of the measured μ_{ep} (Fig. 1) and the calculated Z/r^2 (Fig. 4) points versus Z/r are

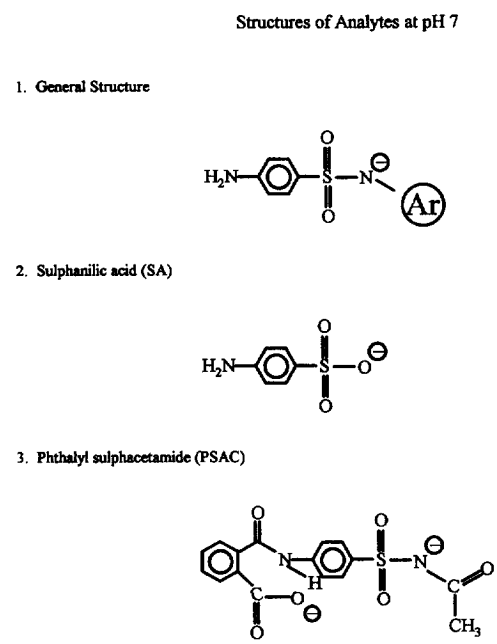

Fig. 3. Structures of analytes at pH 7.

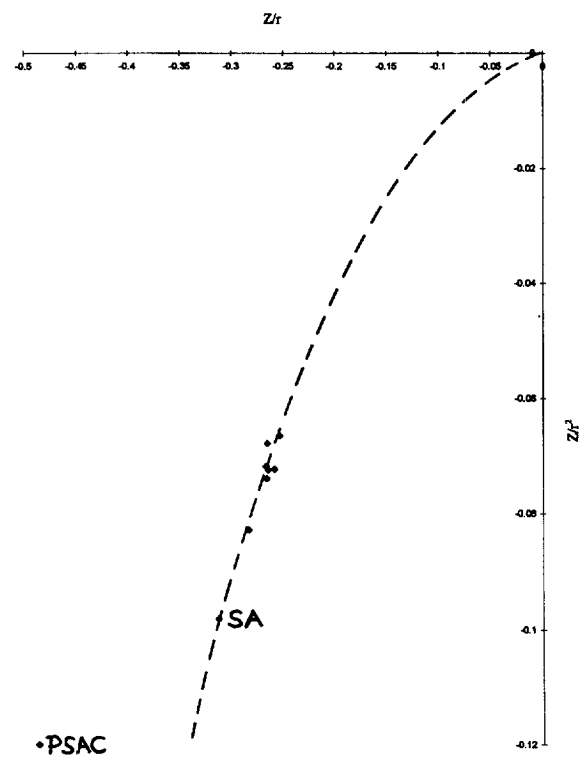

Fig. 4. Z/r^2 plotted versus Z/r for the nine SFAs. The data are taken from Table 1.

strikingly similar and the hand-drawn line of best fit to the Z/r^2 data in Fig. 4 is much like the dashed line in Fig. 1. This strongly suggests that μ_{ep} is related to Z/r^2 rather than Z/r. This comparison also indicates that PSAC is the aberrant analyte and that the line of best fit in Fig. 1 (solid line) is just an average between the dashed line representing the true behaviour and that of PSAC. (The final possible representation of the electrophoretic behaviour of the eight analytes in Fig. 1 (other than PSAC) is a straight line with a physically untenable intercept).

For the four buffer concentrations examined, all plots of μ_{ep} versus Z/r are clearly discriminatory on the basis of size and parabolic dependencies (like the dashed line shown in Fig. 1) are indicative of a higher order dependence upon r. The Z/r^2 plots (Fig. 2, for example) appear linear, have a near zero intercept and are far less size discriminatory.

From the μ_{ep} versus Z/r^3 plot in 174 mM buffer (Fig. 5) it is clear that all size discrimination has

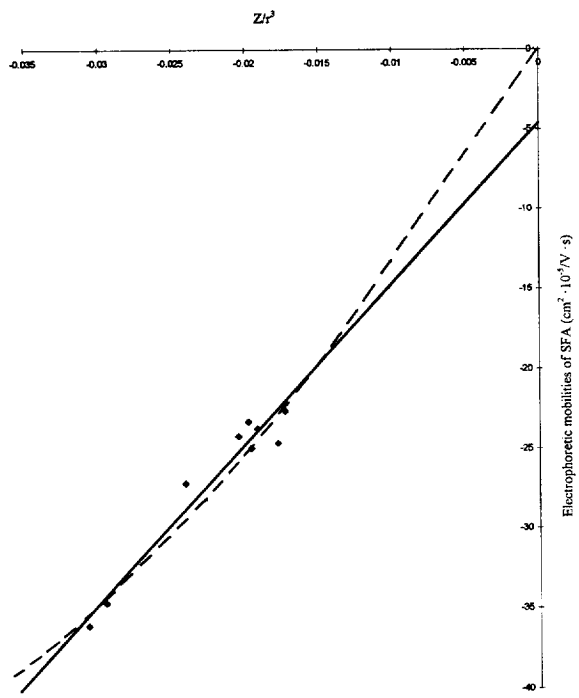

Fig. 5. Electrophoretic mobilities of the nine SFAs ($cm^2 \cdot 10^{-5}$/V s) in 174 mM sodium phosphate buffer plotted versus Z/r^3. The solid line is the linear regression calculated from the experimental results and the dashed line is an alternative interpretation of the data.

disappeared and that this is the tightest fit to the μ_{ep} data. Table 2 confirms this to be equally true at the other three buffer concentrations. The correlation coefficients are significantly higher again, than in the case of Z/r^2. However, in 174 mM buffer (again), the equation to the line of best fit (solid line) is $\mu_{ep}/10^{-5} = -4.736 + 992.0\ Z/r^2$ and from Fig. 5 the magnitude of the intercept is substantial. We would suggest that this is because the true electrophoretic behaviour is best represented by the dashed line, thus indicating a too strong dependence upon r. (Support for this suggestion will be evident in Section 4.2).

4.2. Testing the data of Grossman et al.

The data of Grossman et al. [12] provides an outstanding basis for testing electrophoretic behaviour. The twenty-two peptides range in size from 3–39 amino acid residues (n), in charge (Z) from 1.33 to 14.28 and have Z/n varying from 0.165 to 0.759. For practical purposes, the authors themselves chose to determine the empirical relationship that best described the variation between μ_{ep}, Z and n. The result was $\mu_{ep} = 5.23 \cdot 10^{-4}\ \ln(Z+1)/n^{0.43}$. This expression is a very good fit to the data, so the predictive objective of the research was presumably achieved. However, theoretically it is not very helpful. As mentioned above, Weinberger [3] has suggested that this data may well fit the Compton model [11] in which there is a gradual transition from $1/M_r^{1/3}$ to $1/M_r^{2/3}$ dependence as M_r increases. In Figs. 6–8 the measured μ_{ep} [12] are plotted versus $Z/n^{1/3}$, $Z/n^{2/3}$ and Z/n, respectively.

From Fig. 6 (the μ_{ep} versus $Z/n^{1/3}$ plot), it is immediately obvious that there is a huge scatter of the data and that $Z/n^{1/3}$ badly represents the dependence of the data overall. Linear regression yields a correlation coefficient of 0.62. Furthermore, under the (approximate, solid) line of best fit shown, there is a group of outliers. These are designated by the ■ symbols in Fig. 6. They are the largest analytes ($n \geq 24$) and they form an envelope (dashed line) below and to the right of the rest of the data. In particular, the data for these larger peptides (■) indicate a parabolic or higher order dependence upon $1/n^{1/3}$, perhaps indicating a $1/n^{2/3}$ dependence as has generally been observed for large molecules

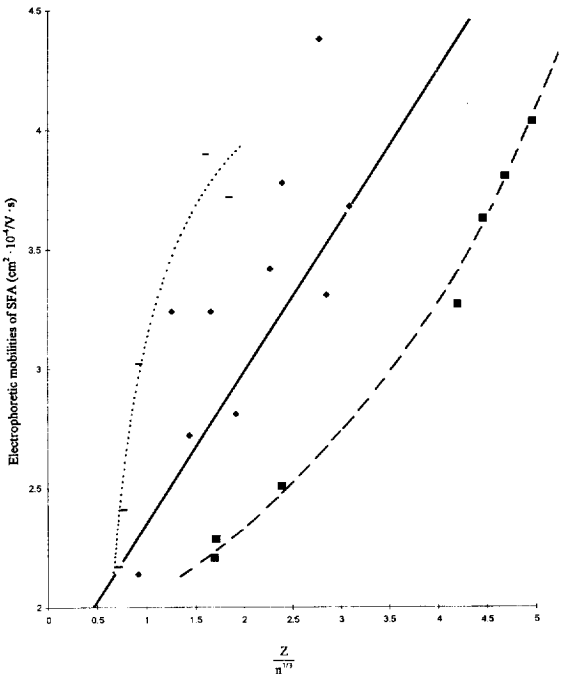

Fig. 6. Electrophoretic mobilities of the twenty-two peptides plotted versus the formal charge (Z, at pH 2.50) over the cube root of the number (n) of amino acid residues. Data taken from Ref. [12]. Legend: (■) largest peptides, (—) smallest peptides, (♦) mid-size peptides. Approximate lines of best fit are drawn to the overall data (solid), the largest peptides (dashed) and the smallest peptides (dotted).

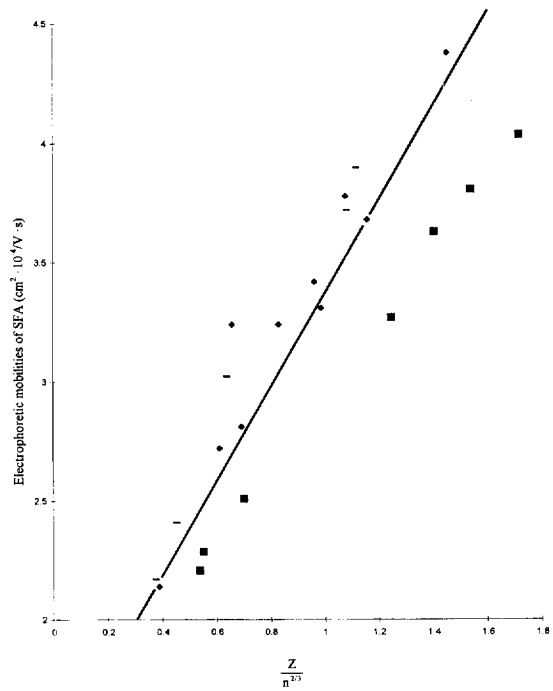

Fig. 7. Electrophoretic mobilities of the twenty-two peptides plotted versus the formal charge (Z, at pH 2.50) over the cube root of the number (n) of amino acid residues, squared. Data taken from Ref. [12]. Legend as for Fig. 6. An approximate line of best fit has been drawn to the data overall.

[5–10]. This could also be consistent with Comptons proposal [11] of a gradual transition in electrophoretic dependencies between $1/n^{1/3}$ for small molecules and $1/n^{2/3}$ for large molecules. The smallest molecules ($n \leq 7$) are designated by the — symbols in Fig. 6 and form an envelope (dotted line) above and to the left of the rest of the data. This limited set of data appear to form a concave shape, but this shape does not greatly alter from Figs. 6–8 in response to $1/n^{x/3}$ increasing from $x = 1$–3. Closer inspection of the plots for this sub-set of the smallest peptides indicates that the relativities change and hence this group should not be taken as a homogeneous set and its behaviour thus overinterpreted. However, the μ_{ep} versus $Z/n^{1/3}$ plot is clearly and strongly discriminatory with respect to size.

Fig. 7 is the μ_{ep} versus $Z/n^{2/3}$ plot. The overall spread of data is considerably reduced ($R = 0.90$) compared to Fig. 6 and each of the individual sets of peptides [small (—), large (■) and intermediate (♦)] have approximately linear plots. However, this plot is again discriminatory with respect to size.

In Fig. 8 (μ_{ep} versus Z/n^1), each of the sets of data points is clearly curved down, indicating that $x = 3$ is too large for μ_{ep} versus $Z/n^{x/3}$ plots.

One further feature of Figs. 6–8 is worthy of note. As x increases from 1–2–3, the data for the large peptides move up to the mean while the plots for the small peptides move down and through the mean. The implication is that somewhere between $x = 2$ and $x = 3$ there is a value which would best represent the data overall. Grossman et al. [12] determined their empirical relationship between μ_{ep}, Z and n by grouping the peptides at fixed charge and determining the dependence upon n. With this fixed, the dependence upon Z was found. Alternatively, setting $\mu_{ep} = A + B \cdot Z \cdot n^{-X}$, rearrangement, followed by taking logarithms, setting $A = 0$, further rearrangement and linear regression would provide a preliminary

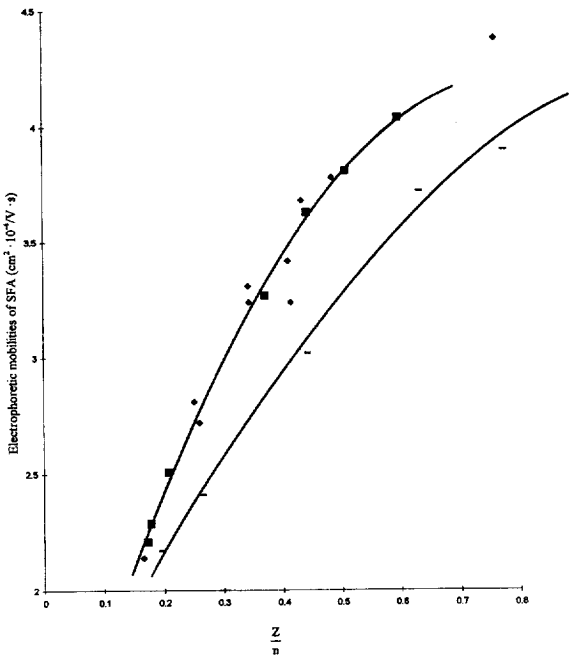

Fig. 8. Electrophoretic mobilities of the twenty-two peptides plotted versus the formal charge (Z, at pH 2.50) over the number (n) of amino acid residues. Data taken from Ref. [12]. Legend as for Fig. 6. Approximate lines of best fit are drawn to the data for the largest peptides (■) and the smallest peptides (—).

estimate of X. Iterations between the given equation and a logarithmic form with rearrangement would then solve the equation. However, an exact value of X between 2/3 and 1 would not be physically meaningful, and, the nature of the data in its present form does not warrant more precise analysis.

Since the data of Grossman et al. [12] is based upon n, the number of amino acid residues linearly linked in the peptides, there will be a significant approximation involved in assuming a direct proportionality between n and M_r and thus the molecular volumes of the peptides. Firstly there are the very large percentage differences between the M_r values and sizes of individual amino acids which could lead to significant scatter in any plotted function of n. Secondly there is the presumption of "linearity". If the peptides all remain extended, one dimension would be properly represented by n. On the other hand, if shape is a determinant of μ_{ep} and peptide conformation is a function of length (and/or sequence), there will be a natural discrimination on the basis of size – as is observed. (A detailed treatment of the effects of shape on translational frictional properties of macromolecules has been given by Cantor and Schimmel [27] and Grossman and Colburn [28] have simplified and summarised the outcomes).

The other important presumption in the analysis of the Grossman et al. [12] data is that the pK_a values of the functional groups on the side chains of the individual amino acids are conserved in the peptide chains. Rickard et al. [10] have demonstrated that this is not the case. Charge modification in the amino acid side chains is significant, as is the effect on correlations between μ_{ep} and $1/M_r^{2/3}$, albeit perhaps only to the extent of halving the scatter in Fig. 7 [29].

5. Summary and conclusions

Two aspects of the electrophoretic migration behaviour have been investigated.

5.1. Theoretical description of electrophoretic migration

(a) By considering migrating ions as their equivalent spheres and assuming distribution of charge over the surface, the electrophoretic mobility is theoretically shown to be dependent upon the square of the reciprocal of the hydrodynamic radius ($1/r^2$), and thus the surface area.

(b) Treatment of the ionic atmosphere as an extended electrical double layer and using the Debye length as the thickness, leads to the known dependence of the electrophoretic mobility upon the square root of the reciprocal of the ionic strength ($1/\sqrt{I}$).

5.2. Testing the dependence of the electrophoretic migration upon the hydrodynamic radius

(i) The electrophoretic mobility data obtained for nine sulphonamide analytes in four buffer concentrations has been shown to support the $1/r^2$ dependence rather than the alternatives of $1/r$ or $1/r^3$ and thereby to support the theoretical relationship derived.

(ii) It is concluded that the data of Grossman et al.

[12] clearly support the dependence of μ_{ep} upon $Z/n^{2/3}$ rather than $Z/n^{1/3}$ or Z/n. Within the constraints of the data, the overall correlation coefficient of 0.899 for the μ_{ep} versus $Z/n^{2/3}$ plot gives a strong indication that μ_{ep} is dependent upon $1/r^2$ (Eq. (6)) and not $1/r$ (Eq. (1)).

Acknowledgments

We thank Dr. Margaret Wong for access to the molecular modelling package and Dr. Ian Harding for helpful discussions. J.C. gratefully acknowledges the receipt of a Swinburne University Postgraduate Research Award, during the tenure of which, some of this work was completed.

References

[1] M.C. Ricci, R.F. Cross, J. Microcol Sep. 5 (1993) 207–215.
[2] J. Cao, R.F. Cross, J. Chromatogr. A 695 (1995) 297–308.
[3] R. Weinberger, in Practical Capillary Electrophoresis, Academic Press, London, 1993, p. 48.
[4] R.F. Cross and J. Cao, Proceedings of the Royal Australian Chemical Institute 13th Symposium on Analytical Chemistry, Darwin, July, 1995, RACI Analytical Chemistry Division, pp. AO18/1–4.
[5] R.E. Offord, Nature (London) 211 (1966) 591–597.
[6] F. Nyberg, M.D. Zhu, J.L. Liao and S. Hjerten, in C. Schaefer-Nielsen (Editor), Electrophoresis '88, VCH, New York, 1988, p. 141.
[7] Z. Deyl, V. Rohlicek, R. Struzinsky, J. Liq. Chromatogr. 12/13 (1989) 2515–2526.
[8] Z. Deyl, V. Rohlicek, M. Adam, J. Chromatogr. 480 (1989) 371–378.
[9] J. Frenz, S.-L. Wu, W.S. Hancock, J. Chromatogr. 480 (1989) 379–391.
[10] C.E. Rickard, M.M. Strohl, R.G. Nielsen, Anal. Biochem. 197 (1991) 197–207.
[11] B.J. Compton, J. Chromatogr. 559 (1991) 357–366.
[12] P.D. Grossman, J.C. Colburn, H.H. Lauer, Anal. Biochem. 179 (1989) 28–33.
[13] R.J. Wieme, in E. Heftmann (Editor), Chromatography – A Laboratory Handbook of Chromatographic and Electrophoretic Method, Van Nostrant Reinhold, New York, 3rd ed., 1975, Ch. 10.
[14] P. Jandik and G. Bonn, in Capillary Elctrophoresis of Small Molecules and Ions, VCH, New York, 1993, p. 61.
[15] H.J. Issaq, I.Z. Atamna, G.M. Muschik, G.M. Janini, Chromatographia 32 (1991) 155–161.
[16] J. Cao and R.F. Cross, submitted for publication.
[17] J.T.G. Overbeek, in H.R. Kruyt (Editor), Colloid Science, Vol. 1, Irreversible Systems, Elsevier, New York, 1952, Ch. V.
[18] R.J. Hunter, in Zeta Potential in Colloid Science – Principles and Applications, Academic Press, London, 1981, p. 69 and App. 2.
[19] A.W. Adamson, in Physical Chemistry of Surfaces, Wiley, New York, 3rd ed., 1976, pp. 179–200.
[20] P.C. Hiemenz, in Principles of Colloid and Surface Chemistry, Marcel Dekker, New York, 2nd ed., 1986, Section 12.4.
[21] I.H. Harding, personal communication.
[22] I.H. Harding, in Colloid Science, Swinburne University Press, Hawthorn, 1995, Ch. 12.
[23] R.A. Robinson and R.H. Stokes, Electrolyte Solutions, Butterworths, London, 2nd ed., 1959, Ch. 4.
[24] R.A. Robinson and R.H. Stokes, Electrolyte Solutions, Butterworths, London, 2nd ed., 1959, Appendix 7.1, p. 468.
[25] Model 270A User's Manual, Applied Biosystems, Santa Clara, CA, 1989.
[26] A. Tiselius, H. Svenssen, Trans. Farad. Soc. 36 (1940) 16–25.
[27] C.R. Cantor and P.R. Schimmel, Biophysical Chemistry, Pt. II, Techniques for the Study of Biological Structure and Function, Freeman, San Francisco, CA, 1980, pp. 555–570.
[28] P.D. Grossman and J.C. Colburn, in Capillary Electrophoresis – Theory and Practice, Academic Press, San Diego, CA, 1992, p. 113.
[29] H.E. Schwartz, R.H. Palmieri and R. Brown, in P. Camilleri (Editor), Capillary Electrophoresis – Theory and Practice, CRC, Boca Raton, FL, 1993, p. 226.